Article

Model-Independent Searches for New Physics in Multi-Body Invariant Masses

Sergei Chekanov [1,*], Smita Darmora [1,*], Wasikul Islam [2,3], Carlos E. M. Wagner [1,4] and Jinlong Zhang [1]

1   HEP Division, Argonne National Laboratory, 9700 S. Cass Avenue, Lemont, IL 60439, USA; cwagner@anl.gov (C.E.M.W.); zhangjl@anl.gov (J.Z.)
2   Department of Physics, Oklahoma State University, Stillwater, OK 74078, USA; wasikul.islam@cern.ch
3   Department of Physics, University of Wisconsin, Madison, WI 53706, USA
4   Physics Department, EFI and KICP, University of Chicago, Chicago, IL 60637, USA
*   Correspondence: chekanov@anl.gov (S.C.); sdarmora@anl.gov (S.D.)

Abstract: Model-independent searches for physics beyond the Standard Model typically focus on invariant masses of two objects (jets, leptons or photons). In this study, we explore opportunities for similar model-agnostic searches in multi-body invariant masses. In particular, we focus on the situations in which new physics can be observed in a model-independent way in three and four-body invariant masses of jets and leptons. Such searches may have good prospects in finding new physics in the situations when two-body invariant masses, which have been extensively explored at collider experiments in the past, cannot provide sufficient signatures for experimental observations.

Keywords: beyond the Standard Model (BSM); invariant mass; jets; leptons; large hadron collider (LHC)

Key Contribution: Model-independent searches in invariant masses in collider experiments.

1. Introduction

In spite of the great effort put into the search for new physics at the Large Hadron Collider (LHC), no signs of physics beyond the Standard Model (BSM) have yet emerged. If BSM physics exists within the reach of the LHC, it is possible that its experimental signatures are more complicated than originally anticipated. A popular method of finding new physics is to study signal-like deviations in two-body invariant masses of jets, leptons or photons, or studies of event rates, assuming that the Standard Model (SM) background rates are well understood in terms of Monte Carlo (MC) simulations or data-driven control regions. However, it is possible that new physics is hidden in complex event signatures, beyond single- and two-particle distributions for which MC simulations may not be reliable and/or have significant uncertainties.

In particle collision experiments, model-independent searches for signal-like deviations in invariant-masses distributions of jets, leptons or photons are typically performed by establishing a background hypothesis representing our best knowledge of the SM. Such expectations can be obtained without MC simulations using data-driven "control regions"; i.e., regions of actual data with similar kinematic features but without BSM events. An alternative approach to the description of shapes of the SM background distribution is to perform a fit of the entire mass spectra with some analytic function or using numeric smoothing techniques. After the background hypothesis is established, searches for BSM physics are performed by looking for deviations above the established background shape. Previous searches for heavy resonances in dijet mass distributions (m_{jj}) using the techniques described above have been performed by ATLAS [1,2] and CMS [3–5].

Model-independent searches using the above-mentioned technique applied to two-body invariant masses are rather popular at the LHC. Only a handful number of LHC

studies [6,7] have gone beyond the two-object mass distributions. In particular, searches in multi-body invariant masses that involve different objects (jets, leptons, photons etc.), without relying on MC predictions, are almost non-existent. In this respect, LHC data have not been fully explored in multi-body invariant masses with the same precision as in published papers with two-body masses.

In this paper, we investigate three and four-body invariant masses for BSM processes. We discuss the importance of such studies when direct observations of BSM signals in two-body decays (i.e., dijets, di-leptons or di-photons) are difficult. The latter can be due to their large width or due to significant backgrounds from inclusive multi-jet QCD events. A typical requirement for the partial width (Γ) and the mass (m) for a heavy particle leading to signals that can be observed in invariant masses using the model-independent approach is $\Gamma/m < 0.2$. Other possible difficulties with two-body invariant masses are a large SM background or small masses ($m_{jj} < 0.5$ TeV) which are difficult to study due to trigger pre-scales [1–5].

Recently, a class of models predicting wide Z' resonances that cannot easily be found using the conventional experimental methods based on two-body invariant masses has been discussed in [8,9]. In this paper, we argue that BSM events with similar broad states coupled to SM fermions can be identified using three and four-body decays.

2. Final State Radiation in BSM Models

Due to a low trigger efficiency for jets with momenta below about 0.5 TeV, two-jet invariant masses are difficult to describe at the LHC using analytic functions or smoothing techniques. As the result of such difficulties, many experimental searches focus on high-mass regions (typically, above 1 TeV). To mitigate the trigger problem for low-mass searches, one can require an associated object that can be used for event triggering. This object can be a photon [10,11] or a jet [12–15] from initial-state radiations.

Particles such as photons and vector-bosons from the final-state radiation of quarks in the decays such as $Z' \to q\bar{q}$ are a valuable option for searches for new physics in two-body invariant masses. In such cases, additional objects from final-state radiation, such as photons or leptons (from W/Z), can be used for both event triggering and for calculations of multi-body invariant masses used in searches. The rate of such events is expected to be significantly lower than that in the inclusive dijet case. The main benefit of such events is in the smoothness of the expected background shape for low masses and the existence of a statistically independent event sample[1] to construct control regions. Experimentally, the inclusion of additional electromagnetic objects (such as leptons l or photons γ) to a dijet invariant mass should not significantly increase the resolution of the reconstructed invariant masses. Therefore, the searches in the masses such as $m_{jj\gamma}$ or m_{jjl} may have advantages for low invariant-mass studies and at least should be considered on an equal footing with the dijet studies.

3. Cascade Decays of BSM Particles

Let us consider several event topologies that have a special property for model-independent BSM searches: such events might be difficult to observe in two-body decays, but many-body decays can exhibit signals that can be detected through observations. To be more concrete, let us consider a cascade decay of a heavy particle A into two other particles B and C. Such decays are typical for the diboson production (for a recent review, see [16]). The most popular channel in experimental searches is when B and C are known bosons (W, Z or H, on-shell or off-shell). Generally, however, A and B may not be known. In the case when B and C are bosons, their two-body decay modes are ether hadronic ($q\bar{q}$) or leptonic ($l^{\pm}\nu$, l^+l^-). To be more specific, we assume that B decays to two jets, while C decays to a lepton and X, where X is another lepton, neutrino or some other particle (detectable or undetectable). This situation is depicted in Figure 1, where the dashed line from the particle C represents such an additional particle.
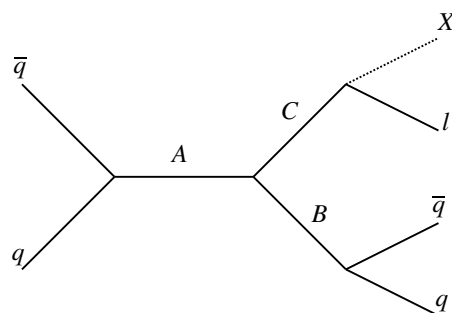
Figure 1. A schematic representation of the decay a heavy particle *A* to two other particles, *B* and *C*.

Searches involving jets and a lepton in the final state that originate from the cascade decays shown in Figure 1 were recently studied [17] by ATLAS using a model-independent approach by triggering on leptons (electrons or muons) and by performing searches in invariant masses, m_{jj}, of two jets. A limitation of such an approach is the width of the heavy particle *B*: if $\Gamma/m > 0.2$, the studies show a small sensitivity to such broad states since such deviations are almost indistinguishable from the background hypothesis.

The studies [17] can be extended by allowing a lepton *l* to participate in the reconstruction of invariant masses. In this case, the three-body invariant masses, m_{jjl}, can be calculated and studied in exactly the same way as the dijet masses m_{jj}. In the situations in which the original particle *A* has a small partial width, the three-body decays can exhibit a narrow signal, which can be sufficient for the observation of this class of BSM processes. Thus, even though particle *B* is not directly observable in dijet decays due to its wide width, the original particle *A* can still be found by observing a deviation on a smooth background distribution using a model-independent approach based on a global fit (or a numeric smoothing technique). Such a class of physics studies has not been extensively explored at the LHC. Below, we illustrate that the expected SM background for three-body decays is indeed a smoothly falling distribution.

3.1. Monte Carlo Simulations

In this section, we illustrate several physics scenarios where three and four-body invariant masses can be a useful tool for observing new physics. For our studies, we use the PYTHIA 8 MC model [18,19] for the generation of *pp*-collision events at $\sqrt{s} = 13$ TeV center of mass energy. Effects from double parton scattering are not included in the simulation. The NNPDF 2.3 LO [20] parton density function from the LHAPDF library [21] was used. Jets, isolated electrons and muons were reconstructed from stable particles. Jets were constructed with the anti-k_T algorithm [22] as implemented in the FASTJET package [23] using a distance parameter of $R = 0.4$. The minimum transverse energy of all jets was 40 GeV in the pseudo-rapidity range of $|\eta| < 2.5$. The leptons are required to be isolated using a cone of the size 0.2 in the azimuthal angle and pseudo-rapidity defined around the true direction of the lepton. All energies of particles inside this cone are summed. A lepton is considered to be isolated if it carries more than 90% of the cone energy. All other details of simulation and reconstruction are described in [29].

3.2. Three-Body Invariant Masses

Let us discuss experimental situations in which three-body invariant masses can be more useful than the usual two-body masses. Three-body invariant masses m_{jjl} reconstructed from two jets and a lepton can be a more powerful variable in the identification of the process $A \rightarrow BC$ than two-body masses under the following conditions:

- Two jets from decays of the particle *B* should be resolved using the standard jet algorithms; see Figure 1. The angular separation of two jets can be approximated by $2m_B/p_T^B$. This implies that the mass of *B* should be comparable with the mass of *A*, such that the particle *B* will not receive a significant boost in transverse momentum; thus, the two jets from the particle *B* can be well resolved.

- The presence of at least one lepton in an event does not set any particular constraints on the mass of C compared to the mass of A. For example, the decay of particle C can be considered fully boosted; i.e., two leptons originating from C will be merged into a single lepton, as seen by experiments. This can happen when the particle C has a significantly smaller mass compared to A; thus, the particle C receives a significant boost in momentum. For TeV scale searches of the particle A, the SM Z boson with the fully boosted decay to l^+l^- can be a possible candidate for C.

  There is another option for this topology: $C \rightarrow l + X$, where X is an undetectable particle, as shown in Figure 1. The particle C can be a W boson, or a BSM boson-like particle, while X can be a neutrino. Such cases also do not impose any restrictions on the mass of C relative to the mass of A.

The above scenarios are convenient for model-independent searches using a data-defined (or phenomenological) smoothly-falling shape for the m_{jjl} distribution if the partial width of A is narrow; i.e., $\Gamma/m < 0.2$. The advantage of searches in m_{jjl}, compared to the direct observation of B in the dijet masses m_{jj}, is most obvious in the case when the partial width of B is large (as in the case of strong decays).

Another possible combination for three-body invariant masses is $j + ll$. If a particle C decays to two resolved leptons, then this type of decay should be detected via the direct searches in di-lepton channels. Thus, this channel should be well covered by the existing LHC studies. On the other hand, if C decays to a highly boosted di-lepton pair, which is resolved as a single lepton, and particle B decays to a jet and lepton, this study can be partially covered by the searches for quantum black holes [25] that use the m_{jl} invariant masses.

4. Specific BSM Models

In this section, we consider several specific BSM models that can be found using three-body invariant masses.

4.1. Models with SM Bosons

A cascade decay of two heavy particles with the associated W gauge boson decaying to $l\nu$ is the natural class of events where multi-body invariant masses are useful for BSM searches. A generic diagram of such processes is shown in Figure 2.
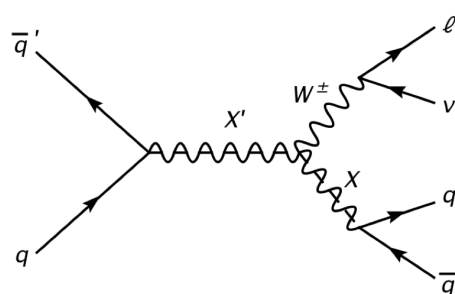

Figure 2. A representative Feynman diagram for a generic resonance, X, decaying to two partons in association with a leptonically decaying W boson in the s-channel. The latter channel includes a resonance X' decaying to a W and an X.

As an example, let us consider the processes $W' \rightarrow WZ' \rightarrow \ell\nu q\bar{q}$ and the $\rho_T \rightarrow W^\pm \pi_T \rightarrow \ell\nu q\bar{q}$ process discussed in [17]. The $W' \rightarrow WZ' \rightarrow \ell\nu q\bar{q}$ and $\rho_T \rightarrow W^\pm \pi_T \rightarrow \ell\nu q\bar{q}$ simulations assume a Z' dijet resonance produced in association with a leptonically decaying W from the $q\bar{q} \rightarrow W'$ process. The mass difference between the W' and Z' was set to 250 GeV. The latter requirement yields the largest predicted cross-section for the desired final state [17].
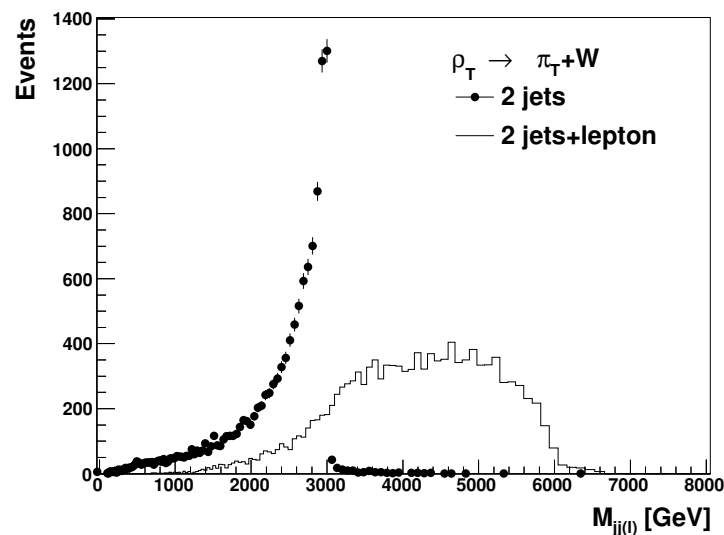
The second process discussed in [17] is $\rho_T \rightarrow W^\pm \pi_T \rightarrow \ell\nu q\bar{q}$. It is a generic technicolor model with a technirho, ρ_T, that decays into a leptonically decaying W boson and a

technipion π_T, decaying into two jets. The mass of the ρ_T is chosen to be larger than the mass of the π_T by a factor of two, which maximizes the cross-section for the $lvq\bar{q}$ final state. These processes are quite distinct kinetically: in one case, the phase space for W production is limited, while it increases with the mass of ρ_T for the technicolor model.

Figure 3 shows the two-jet and two-jet plus lepton invariant masses for the processes discussed above. The processes were simulated and reconstructed as discussed in Section 3. The result shows that there is no principal difference in the width of the two-jet and three-body invariant mass for $W' \rightarrow WZ' \rightarrow \ell v q\bar{q}$. The relative widths of these masses are below 11% (this was estimated by taking the 90% root-mean squared (RMS) value of the distribution and dividing by the mass). Thus, the effect f the missing neutrino is small. This is not the case for $\rho_T \rightarrow W^\pm \pi_T \rightarrow \ell v q\bar{q}$, where the width of the three-body mass is significantly larger than that for the two-jet mass.
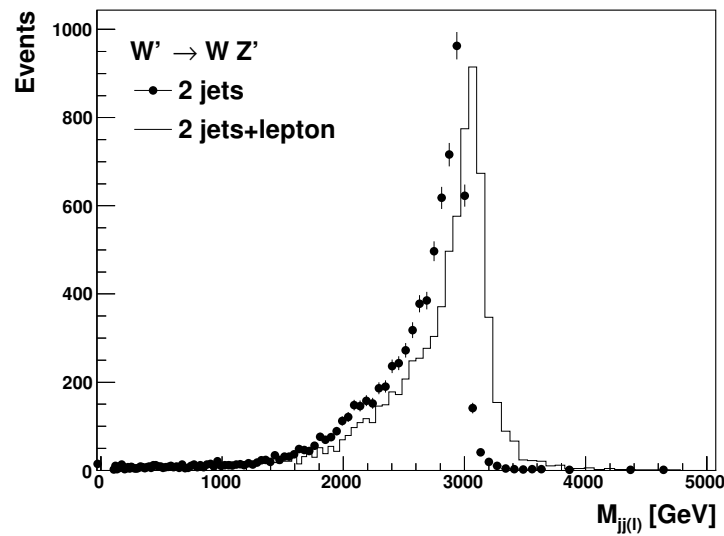
(**a**) W'/Z' SSM model

(**b**) ρ_T model

Figure 3. The invariant masses of two jets (m_{jj}) and two jets and a lepton (m_{jjl}) for (**a**) $W' \rightarrow WZ' \rightarrow \ell v q\bar{q}$ and (**b**) $\rho_T \rightarrow W^\pm \pi_T \rightarrow \ell v q\bar{q}$ process discussed in [17]. The SSM process has a mass splitting between W' and Z' of 250 GeV. The second model has a mass of the ρ_T that is twice as large as that of the π_T.

These examples show that, in some scenarios, such as the first one discussed above, the discovery potential using three-body masses may be as strong as when using the

two-jet masses. Such scenarios belong to the cases when the phase space for production of additional particles, such as *W*, is restricted, and the contribution from the missing neutrino can be approximately ignored. In the unrestricted case, instead, the inclusion of missing energy (MET) from escaping neutrinos leads to broad mass distributions, thus preventing an effective search in smoothly decreasing distributions. Such broad distributions are due to the fact that the reconstructed transverse mass distribution is, in general, much wider than the invariant mass.

4.2. Radion Models

Generally, in order to identify a scenario in which three-body masses have a strong potential for narrow signal signatures, a scan of free parameters needs to be performed. The main tunable parameter is the mass splitting between the two heavy BSM particles. As an example of this scenario, let us consider the following model [26]:

$$W_{kk} \to W + \varphi \to l\nu + gg$$

where W_{kk} denotes the Kaluza–Klein excitation ("KK boson") and φ is a radion particle decaying to two gluons (i.e., jets). Since the *W* bosons decay into $l\nu$, the events should include a ν leading to missing transverse energy (MET). Adding reconstructed MET to the invariant mass reconstruction significantly increases the observed signal width. Therefore, as in the first example in the last section, we explore physics scenarios in which MET is not required (i.e., when the transverse energy of ν is not large).

In this study, we varied the masses of W_{kk} and φ and found a case when the width of the three-body invariant mass is the same as in the case of two-body decays (corresponding to two-jets from the radion). Figure 4a shows the scenario in which the difference in masses between W_{kk} and φ is 250 GeV; i.e., $M_{W_{kk}} - M_\varphi = 250$ GeV. This leads to the width of m_{jjl} being close to the width of m_{jj}.

Another alternative scenario is shown in Figure 4b, where $M_\varphi = M_{W_{kk}}/2$. In the latter case, MET should not be ignored since the neutrino has a significant transverse momentum. It should be noted that, at large W_{kk} masses, the cross-section for the second scenario shown in Figure 4b is a factor 2–5 larger than for the first scenario. However, the benefit of having a narrow signal width for m_{jjl}, leading to large reconstruction sensitivity over a smooth SM background, can compensate for the effects of a lower absolute cross-section. Therefore, the scenario with mass splitting between the two BSM particles close to the mass of associated particles (such as $W/Z/H$) is a preferable configuration for experimental searches in three-body decays.
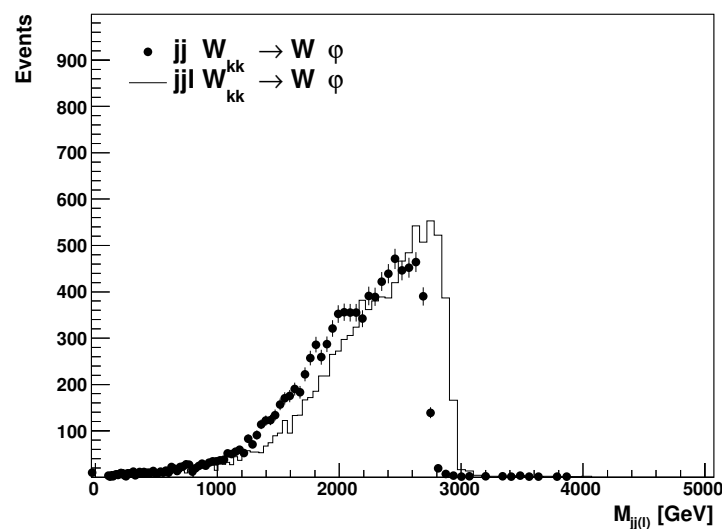
(**a**) Case 1

Figure 4. *Cont.*
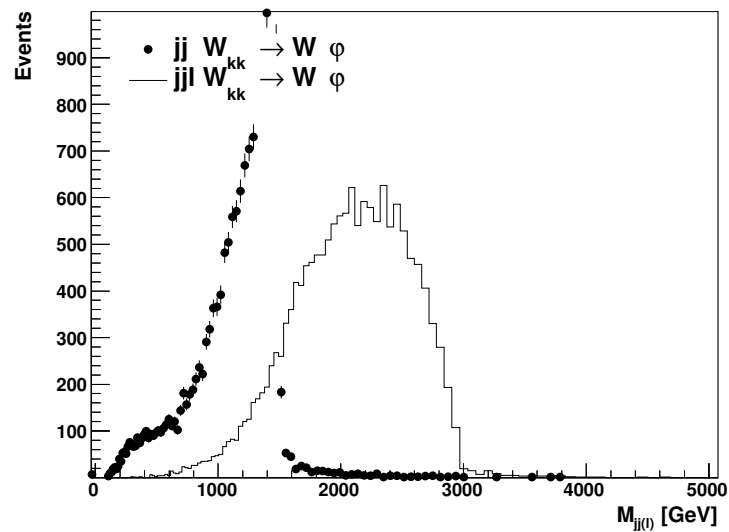
(**b**) Case 2

Figure 4. The m_{jj} and m_{jjl} invariant mass distributions for the 3 TeV Wkk mass when (**a**) case 1 : $M_{W_{kk}} - M_{\varphi} = 250$ GeV & (**b**). Case 2 : $M_{\varphi} = M_{W_{kk}}/2$.

4.3. Composite Resonances

Among different composite resonances models that break lepton flavor (LF) universality, the decay channel $pp \to V \to E^{\pm}l^{\mp}$ (where E is a heavy composite lepton which decays into SM bosons and leptons $E \to Z/h + l$) [27] can easily be probed using the multi-body invariant masses. Figure 5 shows a Feynman diagram for a model where V is a heavy Z' boson ($M(Z') > M(E)$). When Z/h decays hadronically, invariant masses of two jets and a lepton (m_{jjl}) can be used to reconstruct the mass of E. In addition, the 2j + 2l mass (m_{jjll}) is sensitive to the V (Z') mass itself. It should be noted that even if the partial width of the composite E is broad (and thus m_{jjl} is not sensitive to the presence of E), the invariant mass m_{jjll} can still be narrow if the partial width of V is small (which is a typical case for Z').
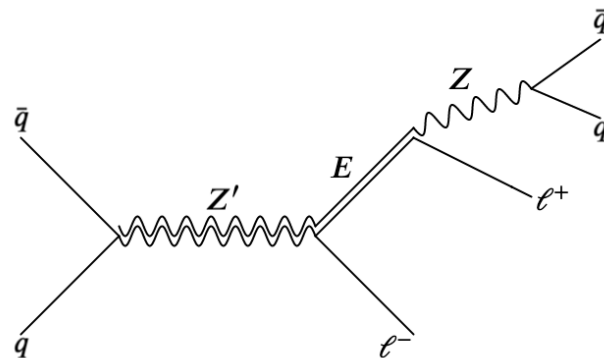

Figure 5. A representative Feynman diagram for the composite lepton model (see Section IV of [27]) where m_{jjl} and m_{jjll} can be used for searches of $V = Z'$ and a composite lepton-like particle E.

Figure 6 shows the m_{jj}, m_{jjl} and m_{jjll} invariant masses reconstructed at the truth level of a Monte Carlo simulation. The selection cuts are set as for the default analysis used in this study. The simulations are performed using Madgraph5 (MG5) [28] with the PYTHIA 8 shower. The masses are set to $M(Z') = 3$ TeV and $M(E) = 2$ TeV in the MG5 simulation. The observed peak near 3 TeV (shown with dotted line) is due to the decay of Z'. The solid line shows two peaks. The largest peak is a reflection of the E decays, while the smaller peak is a reflection of the Z' decays. The two-jet masses show the mass peak at the Z mass, but it has a more complicated distribution than multi-body decays. This figure illustrates that both 2j + l and 2j + 2l invariant masses can be used for searches of events originating from the composite resonances models [27].
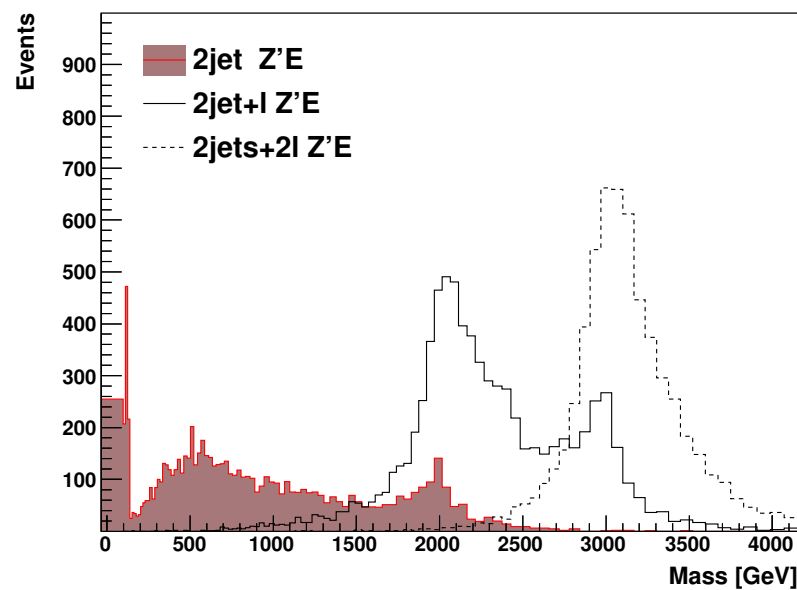
Figure 6. Invariant masses for a $Z'E$ model [27] constructed from two jets, two jets plus a lepton and two jets plus two leptons. The Z' mass was generated at 3 TeV, while $M(E) = 2$ TeV. The simulations were performed using MG5 with PYTHIA 8 showering.

4.4. Hypothetical Scenarios

Based on our analyses in the previous sections, let us consider hypothetical examples in which two-body invariant masses are at a disadvantage for searches since the two-body signal width is larger than three or four-body masses. The goal of such simulation is to illustrate a possible parameter space when two-body masses are less powerful for searching for enhancements on a smoothly falling background than for multi-body masses.

4.4.1. Three-Body Invariant Masses

For the three-body example, we set up a PYTHIA 8 simulations for the process $W' \rightarrow Z'W^*$, where W', Z' and W^* are hypothetical bosons, without assuming any particular physics couplings or model. In this simulation, the mass of W' was set to 1 TeV and its width was set to $\Gamma = 10$ GeV. Z' decays to two jets, while W^* decays to a lepton and a neutrino. The mass of Z' was set to 500 GeV (with $\Gamma = 250$ GeV), and the mass of W^* was set to 300 GeV (with $\Gamma = 250$ GeV). The widths of Z' and W^* in this setup are large ($\Gamma/m \geq 0.5$), and the detection of such particles via the observations of Gaussian-shaped enhancements on smoothly falling m_{jj} distributions is difficult. However, for the m_{jjl} masses, the situation is different. Figure 7 shows that the width of m_{jjl} is smaller than the width of m_{jj} despite the presence of the neutrino that introduces a shift and smearing in the mass distribution. According to this simulation, the relative width of the m_{jjl} masses is close to 15%, which is in the range of acceptable width for the experimental detection on smoothly falling background distributions.
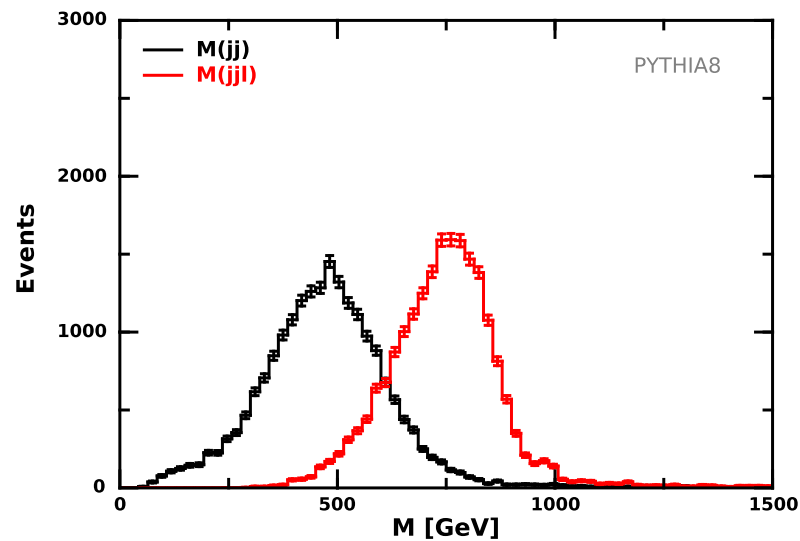
Figure 7. The invariant masses of two jets (m_{jj}) and two jets and a lepton (m_{jjl}) in events $A \to B\,C$ simulated with PYTHIA 8 with the settings described in the text.

4.4.2. Four-Body Invariant Masses

For the four-body decay analysis, consider the example shown in Figure 1, where X could be a lepton or a jet. Hence, events with at least two jets and leptons lead to the following combinations: m_{jjll} and m_{jjjl}. As in the case of three-body decays, model-independent searches for signal-like enhancements in smoothly falling distributions of four-body invariant masses can be simpler than for similar searches in two-body decays when the partial widths of B and C have $\Gamma/m > 0.2$.

Here are possible kinematic scenarios that are not well covered in pp collider experiments:

- Signature searches based on m_{jjll} invariant masses for discovering a TeV-scale particle decaying to two heavy particles when both B and C are heavy; thus, there is no significant momentum boost, and all decay products are well resolved.
- Event topologies contributing to m_{jjjl}, when a particle C decays to a lepton and jets, similar to quantum black hole scenarios [25].

Let us consider a MC simulation for the first scenario. We have created the PYTHIA 8 simulation for the process $W' \to Z'\,W^*$, where W', Z' and W^* are hypothetical bosons. The mass of W' was set to 1 TeV and the width $\Gamma = 10$ GeV. Z' decays to two leptons (electrons or muons), while W^* decays to two jets. The mass of Z' was set to 500 GeV (with the width of 250 GeV), and the mass of W^* was set to 300 GeV (with the width of 150 GeV). Thus, the widths of Z' and W^* are broad, and a detection of such particles via the observations of Gaussian-shaped enhancements in two-body decays is difficult. Figure 8 shows that the relative width of m_{jjll} is smaller than the widths of two-body decays of Z' and W^*. Thus, the relative width of the m_{jjll} distribution due to the W' decays is close to the range for a direct observation of such a state over a smoothly falling background.
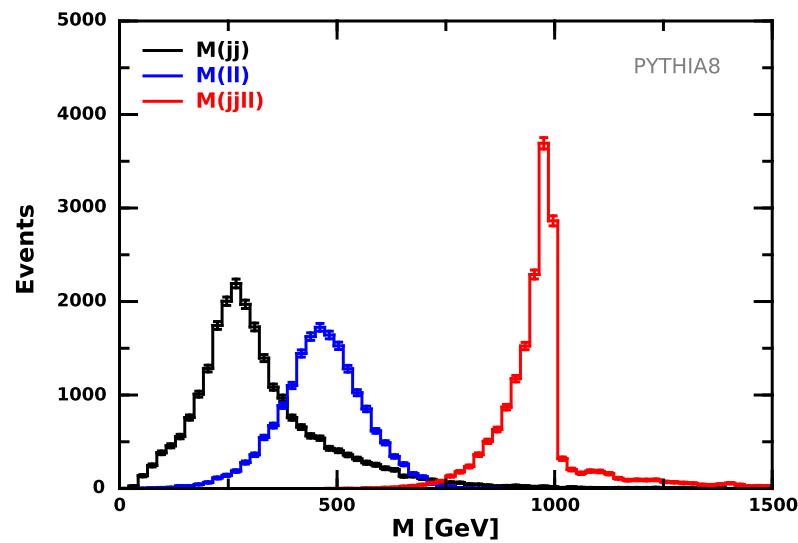
Figure 8. The invariant masses of two jets (m_{jj}), two leptons (m_{ll}) and two jets and two leptons (m_{jjll}) in events $A \to B\,C$ simulated by PYTHIA 8 with the settings as described in the text.

5. Exclusion Limits

Although it would be interesting to derive the limits from four-body invariant masses, such as m_{jjll} or m_{jjjl}, obtaining these limits is difficult due to the lack of experimental publications that can be used to correct Monte Carlo predictions for realistic lepton misidentification rates.

To set upper limits on the observation of a new resonance in the m_{jjl} invariant mass, Monte Carlo simulations have been performed using PYTHIA 8 with settings and object reconstruction as described in Section 3.1. Three SM processes were generated: (1) light-flavor QCD dijets, (2) vector and scalar boson production and (3) $t\bar{t}$. Pileup events were not simulated, but this problem is mitigated by using the normalization factors described below. All other details in the simulation match the description of [24]. Unlike the signal models, the SM background processes require simulations of misidentification rates for muons and leptons ("fake rates"). We used a 0.1% misidentification rate for muons and 1% fake rate for electrons [24]. This was implemented by assigning the probability of 10^{-3} (10^{-2}) for a jet to be identified as a muon (electron) using a random number generator. The distributions were obtained for events with at least one isolated lepton with $p_T^l > 60$ GeV and two jets at $p_T > 30$ GeV. The SM background MC samples are available from the HepSim repository [29].

After the m_{jjl} distributions were reconstructed assuming 140 fb^{-1} separately for muons and electrons, they were scaled to match the official ATLAS Monte Carlo [17].[2] This corrected for residual differences between the truth-level simulations as described above and the ATLAS simulations that included realistic detector effects; i.e., m_{jjl}-dependent lepton misidentification rates and pile-up contributions. The values of the correction were between 2 and 3, depending on m_{jjl}. These values were almost entirely attributed to the correction for the lepton misidentification rates.

Figure 9 shows the invariant masses using three luminosity scenarios: 140 fb^{-1}, 440 fb^{-1} (LHC Run 2+ Run 3) and the HL-LHC (3 ab^{-1} for 14 TeV). The latter distribution was corrected by a correction factor of 12% (estimated using PYTHIA 8) to reflect the change in the CM energy from 13 to 14 TeV. The number of entries per bin was divided by the bin widths. The distributions have smoothly falling shapes, similar to those for the two-body invariant masses studied by ATLAS [1,2] and CMS [3–5]. Therefore, the m_{jjl} distributions can be examined for local excesses above a data-derived estimate of the smoothly falling predictions, which can be obtained using various smoothing techniques or by performing a global fit with an analytic function.
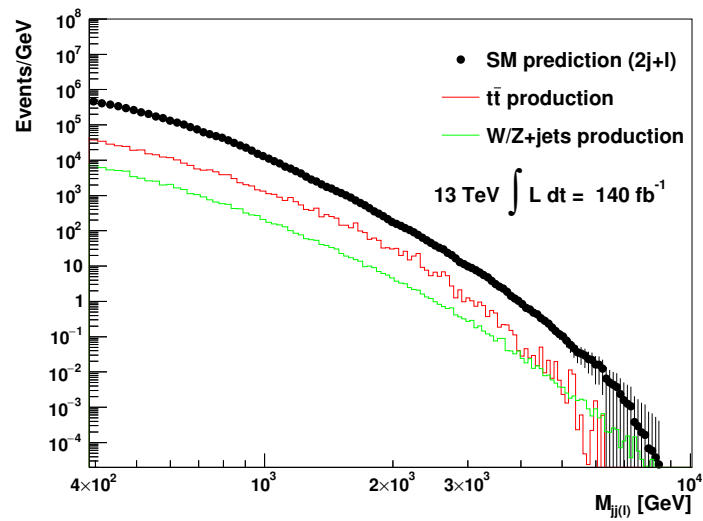
(**a**) 140 fb^{-1}
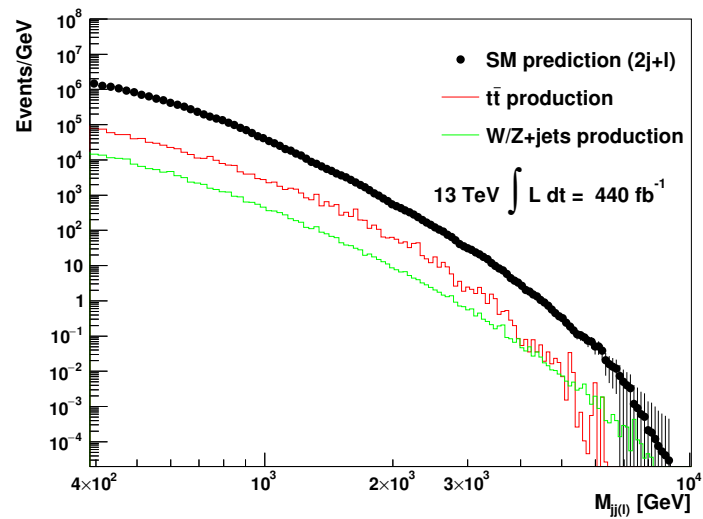
(**b**) 440 fb^{-1}
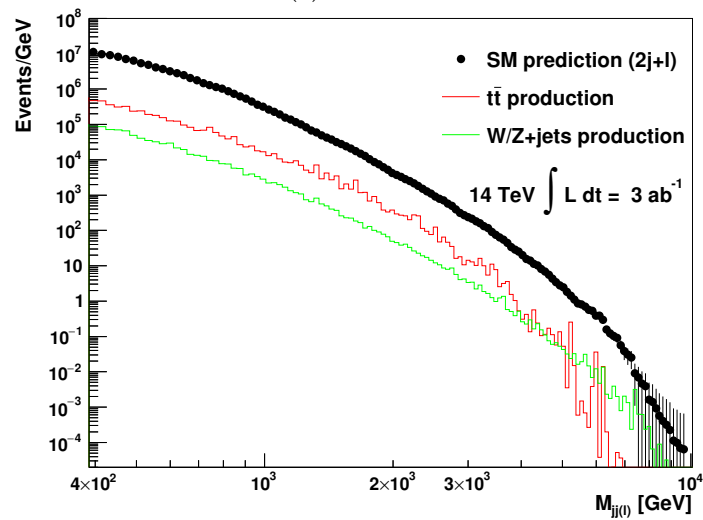
(**c**) 3 ab^{-1}

Figure 9. Expectations for m_{jjl} invariant mass distributions for 140 fb^{-1}, 440 fb^{-1} and 3 ab^{-1} (14 TeV) using the PYTHIA 8 generator for events with at least one isolated lepton with $p_T^l > 60$ GeV. Contributions from $W/Z/H^0$ -boson processes and top-quark processes are shown separately (without stacking the histograms).

Figure 10 shows the expected 95% confidence level (C.L.) upper limit on the fiducial cross-section times the branching ratio for a generic Gaussian signal with the width (σ_G) being 15% of the Gaussian peak position, while decaying to two jets and a lepton. The results are presented for different values of the integrated luminosity, including the luminosity expected after LHC run 3 and high-luminosity LHC. The limits were calculated using the frequentist approach [30] with the asymptotic approximation[3]. The 95% quantile of the posterior was taken as the upper limit on the possible number of signal events in data corresponding to that mass point. This value, divided by the corresponding luminosity, provided the upper limit on the production cross-section of a new particle times the branching ratio (Br) to two jets plus a lepton. The presented limits can be used to estimate the sensitivity of the LHC data to any phenomenological models predicting Gaussian signals in the m_{jjl} distributions.

As emphasized above, the limits for the four-body masses, such as m_{jjll} or m_{jjjl}, are difficult to obtain due to the lack of experimental publications that can be used to correct Monte Carlo predictions for realistic lepton misidentification rates.
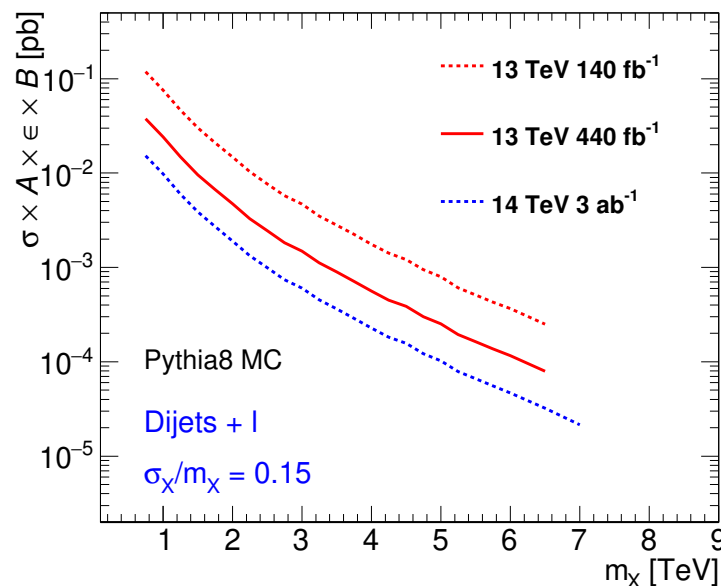
Figure 10. The 95% C.L. upper limits obtained from the m_{jjl} distribution on cross-section times acceptance (A), efficiency (ϵ) and branching ratio (BR), for a BSM signal with a cross-section that produces a Gaussian contribution to the particle-level m_{jjl} distribution, as a function of the mean of the Gaussian mass distribution. The limits are calculated for a BSM signal assuming $\sigma_X/m_X = 0.15$ width.

6. Summary

This paper discusses several scenarios for model-independent BSM searches that have not received sufficient attention in collider experiments. In particular, we focus on generic processes with cascade decays of the type $A \rightarrow BC \rightarrow jjl(l)$, where A is a heavy BSM particle, while either B or C is another heavy particle decaying to jets with a mass smaller than A. For the physics processes discussed in this paper, multi-body invariant masses calculated using two jets and leptons may lead to favorable conditions for experimental observations of signal-like structures on smoothly falling invariant masses. Such structures can be observed with high precision using various smoothing numerical techniques or a global fit of multi-body invariant masses using analytic functions. All methods of this type are widely utilized in dijet searches.

We believe that multi-body final states with leptons are largely unexplored using high-precision model-independent techniques that do not rely on Monte Carlo predictions for SM background. It would be interesting to explore general theoretical scenarios with narrow heavy particles that decay to relatively broad resonances. Such BSM events can easily escape observations using previously published searches in dijets, which are not

the primary observables for such BSM events. Dijet searches in inclusive collision events are also affected by the overwhelming multi-jet QCD background. Therefore, multi-body invariant masses that include leptons have the potential to bring unexpected discoveries. Using Monte Carlo simulations, our analysis set 95% credibility-level upper limits on the signal cross-section times acceptance times efficiency times the branching ratio for new processes that can produce a Gaussian contribution to the dijet plus lepton invariant-mass distribution. The estimated limits can be used to guide model builders, who hypothesize that heavy states lead to signal signatures in such multi-body invariant masses.

The approach described in this paper can equally be applied to invariant masses that include more than four objects or invariant masses that are composed of only jets or leptons. However, such studies are beyond the scope of the current paper.

Author Contributions: Conceptualization, S.C.; Formal analysis, S.D.; Methodology, C.E.M.W.; Project administration, J.Z.; Software, S.C. and W.I.; Visualization, W.I.; Writing—original draft, S.C. and S.D.; Writing—review & editing, S.D. All authors have read and agreed to the published version of the manuscript.

Institutional Review Board Statement: Not applicable.

Informed Consent Statement: Not applicable.

Data Availability Statement: Data available from the HepSim Monte Carlo repository https://atlaswww.hep.anl.gov/hepsim/ (accessed on 7 September 2021).

Conflicts of Interest: The authors declare no conflict of interest.

Notes

1. This independent sample can be constructed after inverting the quality cuts on the electromagnetic object reconstruction.
2. Such distributions are available as additional material from the ATLAS web page of the paper.
3. Due to the approximate nature of this study, we did not take into account systematic effects in the limit calculation. For two-jet plus lepton (or two lepton) invariant masses, systematic uncertainties for exclusion limits are expected to be dominated by jet energy scale and jet energy resolution. Typically, such experimental effects are not significant (i.e., within the 1-sigma band on the limits).

References

1. ATLAS Collaboration. Search for new phenomena in dijet mass and angular distributions from pp collisions at $\sqrt{s} = 13$ TeV with the ATLAS detector. *Phys. Lett.* **2016**, *b754*, 302–322. [CrossRef]
2. ATLAS Collaboration. Search for new phenomena in dijet events using $37\,fb^{-1}$ of pp collision data collected at $\sqrt{s} = 13$ TeV with the ATLAS detector. *Phys. Rev.* **2017**, *D96*, 052004. [CrossRef]
3. CMS Collaboration. Search for dijet resonances in proton–proton collisions at 13 TeV and constraints on dark matter and other models. *Phys. Lett.* **2017**, *b769*, 520–542. [CrossRef]
4. CMS Collaboration. Search for narrow resonances in dijet final states at $\sqrt{(s)} = 8$ TeV with the novel CMS technique of data scouting. *Phys. Rev. Lett.* **2016**, *117*, 031802. [CrossRef]

5.   CMS Collaboration. Search for narrow resonances in the b-tagged dijet mass spectrum in proton-proton collisions at $\sqrt{s} = 8$ TeV. *Phys. Rev. Lett.* **2018**, *120*, 201801. [CrossRef]
6.   CMS Collaboration. Search for Three-Jet Resonances in *pp* Collisions at $\sqrt{s} = 7$ TeV. *Phys. Lett.* **2012**, *718*, 329–347. [CrossRef]
7.   CMS Collaboration. Search for pair-produced three-jet resonances in proton-proton collisions at $\sqrt{s}$ =13 TeV. *Phys. Lett.* **2019**, *99*, 012010. [CrossRef]
8.   Accomando, E.; Coradeschi, F.; Cridge, T.; Fiaschi, J.; Hautmann, F.; Moretti, S.; Shepherd-Themistocleous, C.; Voisey, C. Production of Z'-boson resonances with large width at the LHC. *Phys. Lett.* **2020**, *803*, 135293. [CrossRef]
9.   Li, Y.Y.; Nicolaidou, R.; Paganis, S. Exclusion of heavy, broad resonances from precise measurements of *WZ* and *VH* final states at the LHC. *Eur. Phys. J.* **2019**, *79*, 348. [CrossRef]
10. ATLAS Collaboration. Search for low-mass resonances decaying into two jets and produced in association with a photon using *pp* collisions at $\sqrt{s} = 13$ TeV with the ATLAS detector. *Phys. Lett.* **2019**, *795*, 56–75. [CrossRef]
11. CMS Collaboration. Search for Low-Mass Quark-Antiquark Resonances Produced in Association with a Photon at $\sqrt{s}$ =13 TeV. *Phys. Rev. Lett.* **2019**, *123*, 231803. [CrossRef] [PubMed]
12. Sirunyan, A.M.; Tumasyan, A.; Adam, W.; Ambrogi, F.; Asilar, E.; Bergauer, T.; Brstetter, J.; Brondolin, E.; Dragicevic, M.; Erö, J.; et al. Search for low mass vector resonances decaying into quark-antiquark pairs in proton-proton collisions at $\sqrt{s} = 13$ TeV. *JHEP* **2018**, *1*, 1–41. [CrossRef]
13. CMS Collaboration. Search for Low Mass Vector Resonances Decaying to Quark-Antiquark Pairs in Proton-Proton Collisions at 13 TeV. *Phys. Rev. Lett.* **2017**, *119*, 111802. [CrossRef] [PubMed]
14. CMS Collaboration. Search for low-mass resonances decaying into bottom quark-antiquark pairs in proton-proton collisions at $\sqrt{s} = 13$ TeV. *Phys. Rev.* **2019**, *99*, 012005. [CrossRef]
15. CMS Collaboration. Search for low mass vector resonances decaying into quark-antiquark pairs in proton-proton collisions at $\sqrt{s} = 13$ TeV. *Phys. Rev.* **2019**, *100*, 1–41. [CrossRef]
16. Dorigo, T. Hadron Collider Searches for Diboson Resonances. *Prog. Part. Nucl. Phys.* **2018**, *100*, 211–261. [CrossRef]
17. ATLAS Collaboration. Search for dijet resonances in events with an isolated charged lepton using $\sqrt{s} = 13$ TeV proton-proton collision data collected by the ATLAS detector. *JHEP* **2020**, *6*, 151. [CrossRef]
18. Sjöstr, T.; Mrenna, S.; Skands, P. PYTHIA 6.4 Physics and Manual. *JHEP* **2006**, *5*, 26.
19. Sjöstrand, T.; Mrenna, S.; Skands, P. A Brief Introduction to PYTHIA 8.1. *Comput. Phys. Commun.* **2008**, *178*, 852–867. [CrossRef]
20. Ball, R.D.; Bertone, V.; Carrazza, S.; Deans, C.S.; Del Debbio, L.; Forte, S.; Guffanti, A.; Hartl, N.P.; Latorre, J.I.; Rojo, J.; Ubiali, M. Parton distributions for the LHC Run II. *JHEP* **2015**, *4*, 40. [CrossRef]
21. Buckley, A.; Ferro, J.; Lloyd, S.; Nordström, K.; Page, B.; Rüfenacht, M.; Schönherr, M.; Watt, G. LHAPDF6: Parton density access in the LHC precision era. *Eur. Phys. J.* **2015**, *75*, 1–20. [CrossRef]
22. Cacciari, M.; Salam, G.P.; Soyez, G. The anti-k_t jet clustering algorithm. *JHEP* **2008**, *4*, 63. [CrossRef]
23. Matteo, C.; Gavin, S.P.; Gregory, S. FastJet User Manual. *Eur. Phys. J.* **2012**, *C72*, 1896. [CrossRef]
24. Chekanov, S.V.; Childers, J.T.; Proudfoot, J.; Wang, R.; Frizzell, D. Precision searches in dijets at the HL-LHC and HE-LHC. *J. Instrum.* **2018**, *13*, P05022. [CrossRef]
25. ATLAS Collaboration. Search for Quantum Black Hole Production in High-Invariant-Mass Lepton+Jet Final States Using *pp* Collisions at $\sqrt{s} = 8$ TeV and the ATLAS Detector. *Phys. Rev. Lett.* **2014**, *112*, 091804. [CrossRef]
26. Agashe, K.S.; Collins, J.H.; Du, P.; Hong, S.; Kim, D.; Mishra, R.K. LHC Signals from Cascade Decays of Warped Vector Resonances. *JHEP* **2017**, *5*, 78. [CrossRef]
27. Mikael, C.; Michael, S. Behavior of composite resonances breaking lepton flavor universality. *Phys. Rev.* **2018**, *98*, 035010. [CrossRef]
28. Alwall, J.; Frederix, R.; Frixione, S.; Hirschi, V.; Maltoni, F.; Mattelaer, O.; Shao, H.-S.; Stelzer, T.; Torrielli, P.; Zaro, M. The automated computation of tree-level and next-to-leading order differential cross sections, and their matching to parton shower simulations. *JHEP* **2014**, *7*, 79. [CrossRef]
29. Chekanov, S.V. HepSim: a repository with predictions for high-energy physics experiments. *Adv. High Energy Phys.* **2015**, *2015*, 136093. [CrossRef]
30. Cowan, G.; Cranmer, K.; Gross, E.; Vitells, O. Asymptotic formulae for likelihood-based tests of new physics. *Eur. Phys. J.* **2011**, *71*, 1554. [CrossRef]